DEVELOPMENTAL BIOLOGY

The Hippo pathway coactivator Yorkie can reprogram cell fates and create compartment-boundary–like interactions at clone margins

Joanna C. D. Bairzin, Maya Emmons-Bell, Iswar K. Hariharan*

During development, tissue-specific patterns of gene expression are established by transcription factors and then stably maintained via epigenetic mechanisms. Cancer cells often express genes that are inappropriate for that tissue or developmental stage. Here, we show that high activity levels of Yki, the Hippo pathway coactivator that causes overgrowth in *Drosophila* imaginal discs, can also disrupt cell fates by altering expression of selector genes like *engrailed* (*en*) and *Ultrabithorax* (*Ubx*). Posterior clones expressing activated Yki can down-regulate *en* and express an anterior selector gene, *cubitus interruptus* (*ci*). The microRNA *bantam* and the chromatin regulator Taranis both function downstream of Yki in promoting *ci* expression. The boundary between Yki-expressing posterior clones and surrounding wild-type cells acquires properties reminiscent of the anteroposterior compartment boundary; Hedgehog signaling pathway activation results in production of Dpp. Thus, at least in principle, heterotypic interactions between Yki-expressing cells and their neighbors could activate boundary-specific signaling mechanisms.

INTRODUCTION

As an organism develops from a fertilized egg, different portions of the embryo begin to exhibit specific patterns of gene expression. Those patterns of gene expression could be a consequence of the position of those cells in the embryo (e.g., Hox genes) or the specification of cells to the primordia of specific tissues (e.g., Pax6 for eye precursors). These patterns of gene expression are initially established by the expression of a specific combination of transcription factors and then stabilized by the attainment of specific chromatin states that make some genes more accessible to the transcription machinery, the so-called epigenetic landscape (*1*, *2*).

For many years, cancer cells have been known to display morphological characteristics that are inappropriate to their tissues of origin. One possible explanation is that cancer cells express tissue-inappropriate genes (*3*, *4*). Recent efforts at characterizing genomes of cancers have shown that a subset of human cancers have mutations in chromatin regulators and splicing factors, which would be predicted to cause changes in gene expression or alterations in the expression of certain splice isoforms (*5*). However, it is also possible that the activation of a variety of oncogenes or inactivation of tumor suppressor genes could themselves cause tissue-inappropriate gene expression. Currently, we have a poor understanding of how oncogenesis can perturb mechanisms that preserve tissue-specific patterns of gene expression and the biological consequences of these perturbations.

The mechanisms that function during development to establish region-specific and tissue-specific patterns of gene expression have been studied extensively in *Drosophila*. A hierarchy of transcription factors acts during early embryogenesis to set up patterns of selector gene expression that specify individual regions of the embryo. Examples include the Hox gene *Ultrabithorax* (*Ubx*), which is expressed in specific embryonic segments, and the genes *engrailed* (*en*) and *cubitus interruptus* (*ci*), which are expressed in the posterior and anterior compartments of each segment, respectively. Once their patterns of expression are established, they are maintained by epigenetic mechanisms that include the involvement of the Polycomb and Trithorax groups of genes (*6*).

The pathways that promote tissue growth are conserved between humans and *Drosophila*. In *Drosophil*a imaginal discs, the larval primordia of adult structures such as wings and eyes, increased activity of growth-promoting pathways can result in tissue overgrowth. This overgrowth can be elicited by expressing Myc (*7*), an activated form of Ras (RasV12) (*8*, *9*), or Yorkie (Yki) (*10*), the coactivator downstream of the Hippo pathway [reviewed in (*11*)] in clones of cells. This allows us to investigate the effects of each of these genes on the patterns of selector gene expression that have been established in the imaginal discs.

Here, we show that among the genes tested, an activated form of Yki (yki^{CA}) is especially potent in destabilizing established patterns of selector gene expression. Clones of yki^{CA} cells in the posterior compartment of the wing disc express the anterior selector gene *ci* instead of the posterior gene *en* and sometimes inappropriately express *Ubx*. We present an investigation of these changes and also show that heterotypic interactions at the boundary between the overgrown clone and surrounding wild-type cells can acquire properties reminiscent of a compartment boundary, a phenomenon that could potentially occur at tumor margins in general.

RESULTS

To test whether oncogenes can also affect the stability of selector gene expression, we created clones of cells expressing either *Myc* (*7*), an activated form of *Ras* (*RasV12*) (*8*), or an activated form of *yki* (yki^{CA}) with a mutation in its critical serine-168 phosphorylation site, which negatively regulates nuclear localization (*10*, *12*, *13*) in the wing imaginal disc. In third instar wing discs, Ci is expressed only in cells anterior to the compartment boundary (Fig. 1A), and Ubx is expressed in the squamous cells of the peripodial epithelium (Fig. 1B) but not in the disc proper. In discs containing multiple yki^{CA}-expressing clones, we found clones in the posterior (P) compartment expressing Ci (74 of 76 discs) and clones in the disc proper expressing Ubx (23 of 28 discs)

Department of Molecular and Cell Biology, 515 Weill Hall, University of California, Berkeley, Berkeley, CA 94720, USA.
*Corresponding author. Email: ikh@berkeley.edu

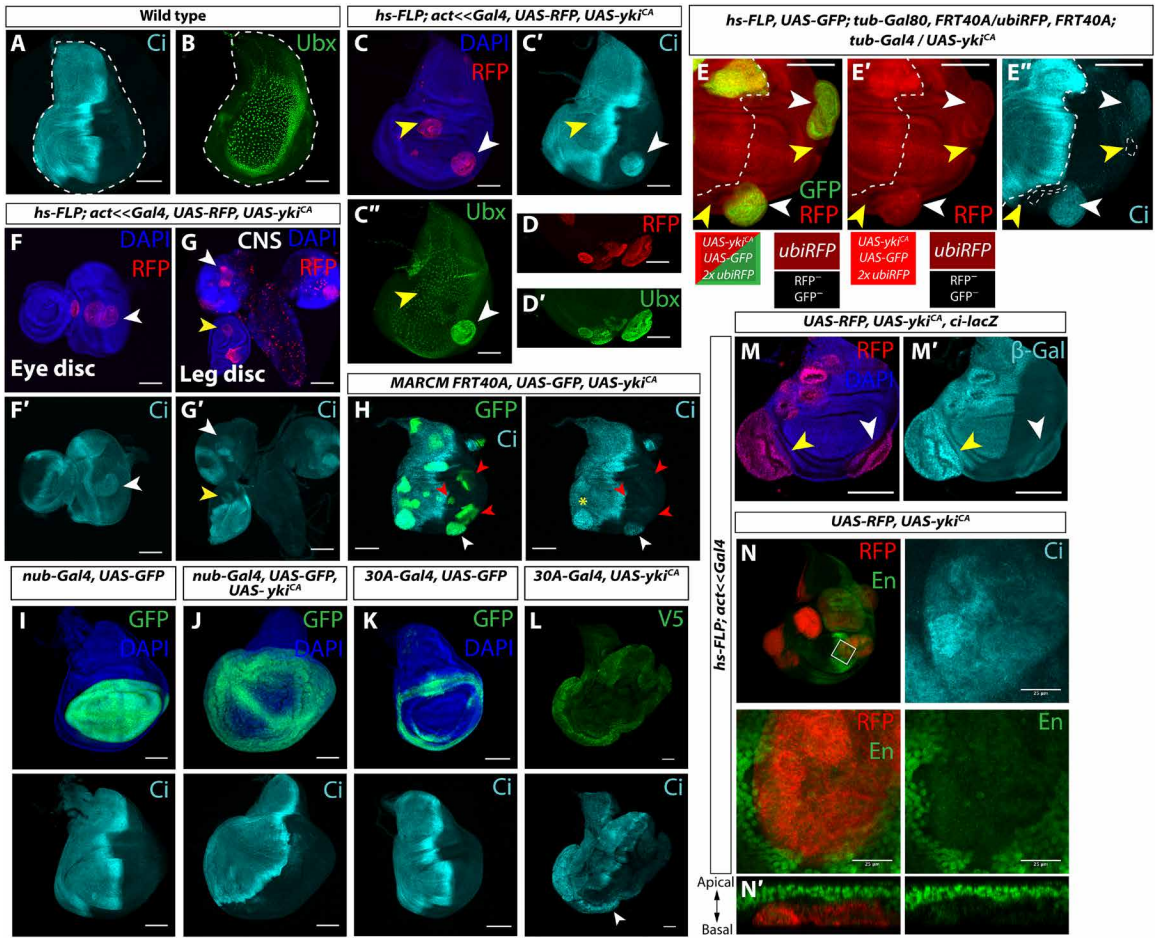

Fig. 1. Constitutively active Yorkie (Yki^{CA}) disrupts stable selector gene expression. (**A** and **B**) Wild-type (WT) wing imaginal discs; Ci is expressed in anterior compartment, and Ubx is expressed in squamous peripodial cells. (**C** to **C″**) Clones expressing activated Yki (*UAS-yki^{CA}*). Anterior clone (yellow arrowhead) expresses more Ci; posterior clone (white arrowhead) expresses ectopic Ci and Ubx (C″). Discs with Ci-positive clones: $n = 74$ of 76. Discs with Ubx-positive clones: $n = 23$ of 28. (**D** and **D′**) Ubx-expressing *yki^{CA}* clones in the disc proper. (**E to E″**) Mitotic recombination: *yki^{CA}*-expressing clones express red fluorescent protein (RFP) and green fluorescent protein (GFP) (white arrowheads), and neighboring twin spots (yellow arrowheads) express neither. (**F** and **G**) *yki^{CA}* clones in the eye disc (F and F′), leg disc [(G) and (G′), yellow arrow], and larval brain [(G) and (G′), white arrow]. CNS, central nervous system. (**H**) Posterior *yki^{CA}* marked with GFP expresses Ci in the hinge (white arrowhead) but inconsistently in the pouch (red arrowheads). Anterior clones express more Ci (yellow asterisk). (**I** to **L**) *nubbin-Gal4, UAS-yki^{CA}* does not cause ectopic Ci [(J), marked by GFP, control disc in (I)], but *30A-Gal4 UAS-yki^{CA}* does [(L), V5 tag on Yki^{CA}, control disc in (K)], especially in the ventral hinge (arrowhead). (**M** and **M′**) *ci-lacZ* is expressed in posterior clones (white arrowheads), and expression is increased in anterior clones (yellow arrowheads). (**N**) A posterior *yki^{CA}* clone with down-regulated En and ectopic Ci expression. (**N′**) *XZ* section of a posterior *yki^{CA}* that has been extruded basally. Anterior is left in all images. Scale bars, 100 μm. DAPI, 4′,6-diamidino-2-phenylindole; β-Gal, β-galactosidase.

(Fig. 1, C and D). Ectopic expression of two other Hox genes *Antennapedia* and *Abdominal-B* was not observed in these clones. Many of these clones appear to be extruding from the epithelium, as has been described when patterning gene expression has been altered within clones of cells (*14*–*16*). To rule out the possibility that the posterior Ci-expressing clones had originated in the anterior (A) compartment, we generated *yki^{CA}* clones using mitotic recombination that marked both the *yki^{CA}*-expressing clone and its wild-type sister clone. We observed Ci-expressing *yki^{CA}* clones in the posterior compartment adjacent to wild-type twin spots, thus confirming that they originated in the posterior compartment (Fig. 1, E to E″). We did not observe a similar misexpression of these genes in discs expressing either *Myc* or *RasV12* (fig. S1, A, A′, B, B′, and C). Thus, of the oncogenes tested, *yki* appears especially capable of altering expression patterns of selector genes. We also observed Ci expression in *yki^{CA}* clones posterior to the morphogenetic furrow in the eye disc (Fig. 1F), in the posterior compartment of the leg disc, and in the central nervous system (Fig. 1G), indicating that *yki^{CA}* can promote Ci expression in diverse tissues. In addition to ectopic expression of Ci, we sometimes observed elevated Ci expression in tissues where Ci is normally expressed, such as in clones in the anterior compartment of the wing disc (Fig. 1, C and H).

The induction of ectopic Ci expression was not observed in clones overexpressing wild-type *yki* or clones mutant for the Hippo pathway components *hippo* (*hpo*) or *warts* (*wts*), (fig. S1, D to F). Thus, ectopic Ci expression depends on especially high levels of Yki activity, caused by overexpression of a form of Yki that cannot be inhibited by Hpo and Wts and hence localizes efficiently to the nucleus. Furthermore, observing clones at different stages of development indicated that ectopic Ci expression required prolonged expression of

yki^{CA} (fig. S2). Even within a given tissue, we observed regional differences in the level of ectopic Ci expression. In the wing disc, clones in the hinge typically expressed higher levels of Ci than clones in the pouch (Fig. 1H). When *yki*^{CA} was expressed using *nub-Gal4*, which is mostly expressed in the pouch, relatively little ectopic Ci was observed (Fig. 1, I and J). In contrast, when the hinge driver *30A-Gal4* was used, ectopic Ci was consistently observed, especially in the ventral hinge posterior to the compartment boundary (Fig. 1, K and L). The hinge is a region of the disc that displays increased plasticity following damage and can be a tumor "hotspot" (*17*, *18*), suggesting that the underlying cause of these phenomena may be related.

ci is normally transcribed exclusively in anterior cells of the wing disc and is repressed in posterior cells by *en* (*19*–*21*). Clones of posterior cells that are mutant for both *en* and its adjacent paralog *invected* (*inv*) express Ci (*19*). Posterior *yki*^{CA} clones up-regulate a transcriptional *ci* reporter, *ci-lacZ*, indicating that *ci* transcription is derepressed (Fig. 1M). Large Ci-positive posterior clones have reduced levels of staining with antibody 4D9, which recognizes both En and Inv (*22*), suggesting that the derepression of *ci* transcription could result from a reduction in En and Inv levels (Fig. 1N). En has also been shown to negatively regulate *Ubx* expression in the wing disc, although that mechanism is less well defined (*23*, *24*); consistent with this, we only observed ectopic Ubx in posterior *yki*^{CA} clones. Since Ci is expressed at elevated levels in anterior clones, where En is not normally expressed, *yki*^{CA} must also be capable of regulating *ci* expression by mechanisms that are independent of changes in En levels. Consistent with this notion, *ci* was identified as a Yki target, and ci RNA was elevated in tissue mutant for *wts*, which has higher Yki activity than wild-type tissue (*25*).

How does Yki regulate *ci* expression? Yki acts together with its binding partner Scalloped (Sd) to activate gene expression, with Sd binding directly to regulatory regions of target genes (*26*). If Sd is the relevant binding partner, then alterations in gene expression would not occur in Yki-expressing clones that are mutant for *sd* (*27*). To determine whether Sd is required for expression of *ci*, we reduced *sd* expression in *yki*^{CA} clones (Fig. 2, A to I). Anterior *yki*^{CA} clones did not show increased Ci expression (Fig. 2, D to F, G to G″, and H to H″), while posterior *yki*^{CA} clones no longer expressed ectopic Ci (Fig. 2, D to F and I to I″), indicating that Sd is required for ectopic Ci up-regulation. Yki promotes growth, in large part, by activating expression of the microRNA *bantam* (*ban*) (*28*–*30*). To address a possible role for *ban* in mediating ectopic *ci* expression, we reduced ban levels by generating *yki*^{CA} clones in flies heterozygous for a null allele of *ban*, *ban*$^{\Delta 1}$ (Fig. 2, J and K; control in fig. S3A) (*31*). In *ban*$^{\Delta 1}$/+ discs, discs appeared smaller overall, although clone size was unaffected (Fig. 2Q), yet the frequency of Ci-expressing *yki*^{CA} clones was reduced both overall and especially in the hinge (Fig. 2R). Thus, the ability of constitutively active Yki (Yki^{CA}) to activate Ci expression in posterior clones is more sensitive to *ban* levels than its ability to promote overgrowth. We also used a "bantam sponge," which encodes an RNA that has 10 optimal *ban*-binding sites upstream of the DsRed coding region; low DsRed expression likely correlates with clones with higher *ban* levels (*32*). We found that clones expressing high levels of DsRed had low Ci levels and vice versa, suggesting a correlation between *ban* levels and induction of Ci (Fig. 2, L and M).

We also investigated *taranis* (*tara*), originally classified as a TrxG gene, which is known to modulate homeotic gene expression by hitherto undefined mechanisms (*33*). A genome-wide chromatin immunoprecipitation screen for Yki targets found an enrichment of Yki binding in the *tara* promoter, as well as increased *tara* transcription in *wts*^{P2} discs (*25*). There is a putative binding site for Sd, Yki's primary binding partner, approximately 400 base pairs upstream of the *tara* transcriptional start site. In addition, *tara* negatively regulates *en* expression in embryos and in regenerating imaginal discs (*34*, *35*). We found that Taranis protein levels were increased in *yki*^{CA}-expressing clones, as was the expression of a *tara-lacZ* transcriptional reporter (Fig. 2, N and O). These findings are consistent with the possibility that an increase in Taranis in *yki*^{CA} clones reduces En levels and thus allows Ci expression. To examine this possibility, we reduced *tara* expression in *yki*^{CA} clones (Fig. 2P; control in fig. S3B). These clones were slightly larger than *yki*^{CA} clones (Fig. 2Q), but the expression of ectopic Ci was reduced (Fig. 2R). This result implicates *tara* in the pathway by which Yki^{CA} induces Ci expression and also shows that ectopic Ci expression does not simply correlate with the extent of overgrowth.

Since our results implicate both *ban* and *tara* in the pathway by which Yki^{CA} activates ectopic Ci expression, we tested whether increasing *ban* and *tara* levels, either alone or in combination, could induce Ci expression in the posterior compartment. Posterior clones overexpressing either *ban* or *tara* alone in wild-type discs expressed very low levels of Ci at most (fig. S3, D and E). However, when expressed in combination with a wild-type version of *yki*, which normally does not induce Ci expression (fig. S3C), either *ban* or *tara* could induce Ci expression, especially in the posterior ventral hinge (Fig. 3, A and B). *tara* overexpression also enhanced Ci expression in Yki^{CA} clones (Fig. 3C).

Furthermore, clones expressing *ban* and *tara* together could induce ectopic Ci at a low frequency and cause overgrowth reminiscent of *yki*^{CA} overexpression (Fig. 3D); anterior clones expressed a higher level of Ci than surrounding wild-type tissue (Fig. 3E). Clones expressing both *tara* and *ban* did not have an obvious decrease in En expression (Fig. 3E′), although a reduction in *tara* has previously been linked to result in increased En expression (*34*, *35*). Thus, *tara* likely regulates *ci* expression independently of *en*. We also found that anterior clones expressing *ban* and *tara* expressed ectopic En (Fig. 3E′), thereby generating clones that coexpress Ci and En, which indicates that, at least in this situation, the mere presence of En is insufficient to repress Ci expression and that *tara* in combination with *ban* can destabilize selector gene expression in multiple ways. When using the hinge *30A-Gal4* driver, combined expression of both *ban* and *tara*, but not either alone, induced a low but reproducible level of posterior Ci and Ptc expression in wild-type discs (fig. S3, H and I; control in fig. S3, F and G). The lower levels of ectopic Ci expression when compared to *yki*^{CA} clones and the absence of En down-regulation elicited by *ban* and *tara* coexpression indicate that Yki^{CA} must also act via additional unidentified targets. Consistent with this idea, overexpression of *ban* and *tara* together in *yki*^{WT} clones recapitulated the *yki*^{CA} clone phenotype to a greater extent, with consistent although often low-level ectopic Ci expression (Fig. 3F). A total of 77.2% of clones expressing Yki^{WT} in combination with *ban* and *tara* expressed ectopic Ci versus 34.6% of clones expressing just *ban* and *tara* (Fig. 3G). In addition, while *tara* overexpression induced *ban* expression as assessed by a *ban-GFP* reporter (fig. S3, J and K) (*28*), *ban* overexpression did not induce *tara* (fig. S3, L and M), indicating that the increase in Tara levels does not result from the known ability of Yki to activate *ban* expression.

To look for evidence of alterations in chromatin in *yki*^{CA} clones, we used a panel of antibodies that recognize specific posttranslational

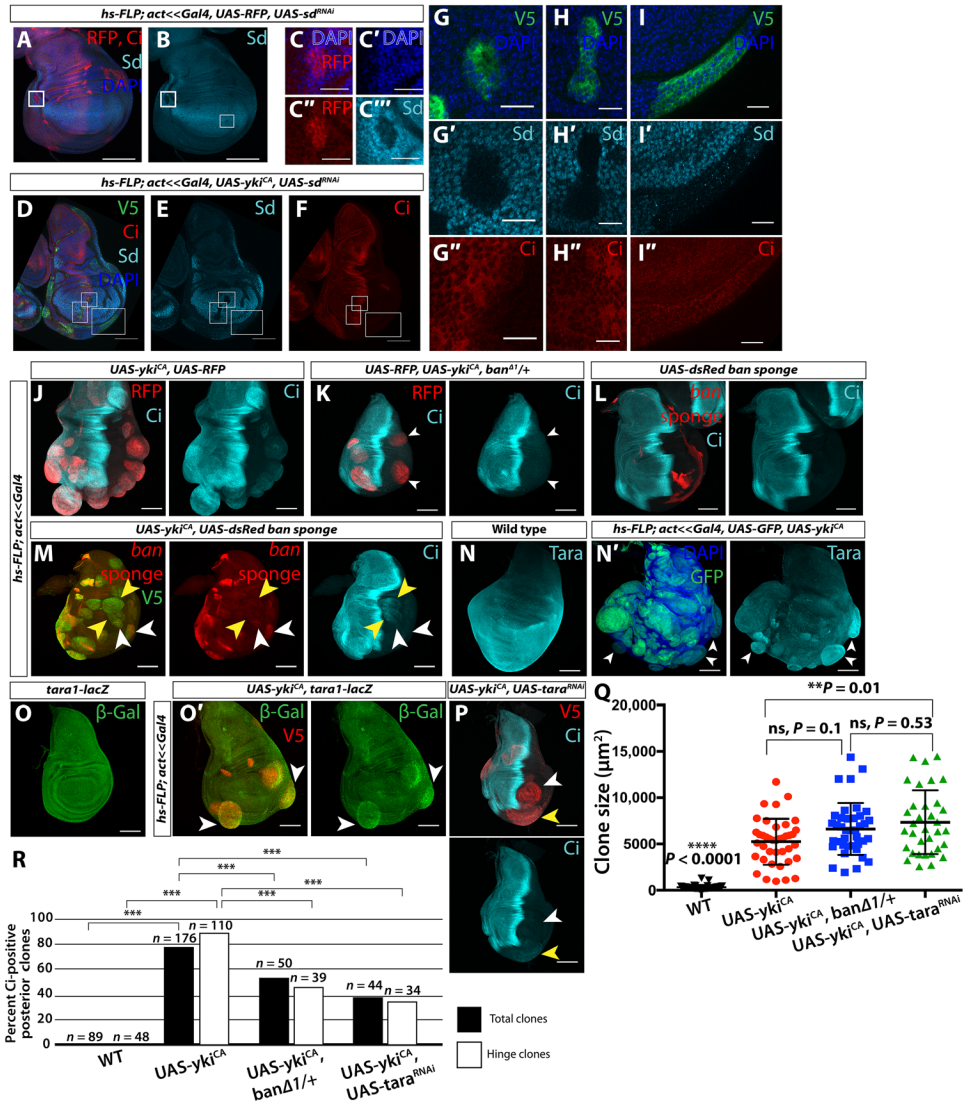

Fig. 2. *yki*^{CA} clones require *sd*, *ban*, and *tara* to disrupt patterning gene expression. (**A** to **I**) RNA interference (RNAi) of *sd* [validated in (A) to (C‴) using anti-Sd] in anterior *yki*^{CA} clones prevents increased Ci expression (D to F, G to G″, and H to H″) and Ci expression in posterior clones (D to F and I to I″). (**J** and **K**) *yki*^{CA} clones in *ban*$^{\Delta 1}$/+ discs (K) are overgrown but express less ectopic Ci [compared to (J)]. (**L** and **M**) *ban* sponge reduces *ban* microRNA levels. dsRed levels inversely correlate with *ban* levels. Clones expressing *ban* sponge express uniformly high dsRed and no ectopic Ci (L). Posterior clones expressing Yki^{CA} and *ban* sponge show variation in both dsRed and Ci expression (M). High dsRed-expressing posterior clones are smaller and do not express Ci (white arrowheads); low- or no-dsRed clones are overgrown and express Ci (yellow arrowheads). (**N** and **O**) Yki^{CA} clones have increased expression of Tara protein (N and N′) and *tara1-lacz* (O and O′), especially in the hinge (arrowheads). (**P**) *tara* RNAi allows overgrowth but reduces Ci expression. (**Q**) Size of posterior hinge clones of indicated genotypes. *yki*^{CA} clones in *ban*$^{\Delta 1}$/+ discs are not significantly smaller than those in WT discs; *yki*^{CA} + *tara*^{RNAi} clones are significantly larger than *yki*^{CA} clones. (**R**) Ectopic Ci is observed less often in *yki*^{CA} clones when *ban* or *tara* levels are reduced. White boxes, hinge clones; black boxes, hinge and pouch clones. Statistics: See Materials and Methods. ns, not significant.

modifications of histones. We found that *yki*^{CA} clones, especially in the hinge, show elevated levels of H3K27 trimethylation (H3K27me3), which typically correlates with increased Polycomb group (PcG)–mediated gene repression (Fig. 3H) (*36*, *37*). We observed less obvious increases in the level of H3K4me1 and H3K4me3, but not H3K9me3 or H4Ac (fig. S4, A to D). The increase in H3K27me3 could potentially explain the decrease in En expression in *yki*^{CA} clones. However, the expression of *en* in the posterior compartment of imaginal discs is regulated by a particularly large region (approximately 79 kB) (*38*) composed of multiple regulatory elements that sometimes function antagonistically, which makes it difficult to evaluate the relevance of local alterations in H3K27me3. The apparent global increase in H3K27me3 levels did not always correlate with increased PcG-mediated repression; a reporter that is silenced by a Polycomb (Pc)-responsive element from the *bxd* locus (*39*) is derepressed in *yki*^{CA} clones (Fig. 3I). Thus, the effects of Yki^{CA} on chromatin state appear to be complex, and hence, effects on individual genes are not easy to predict. This is consistent with the notion that *yki*^{CA} activates Ci expression by multiple mechanisms, as demonstrated by effects on Ci in both anterior and posterior compartments.

To test whether the increases in *tara* and H3K27me3 expression are specific to Yki^{CA} activation or whether these phenomena occur

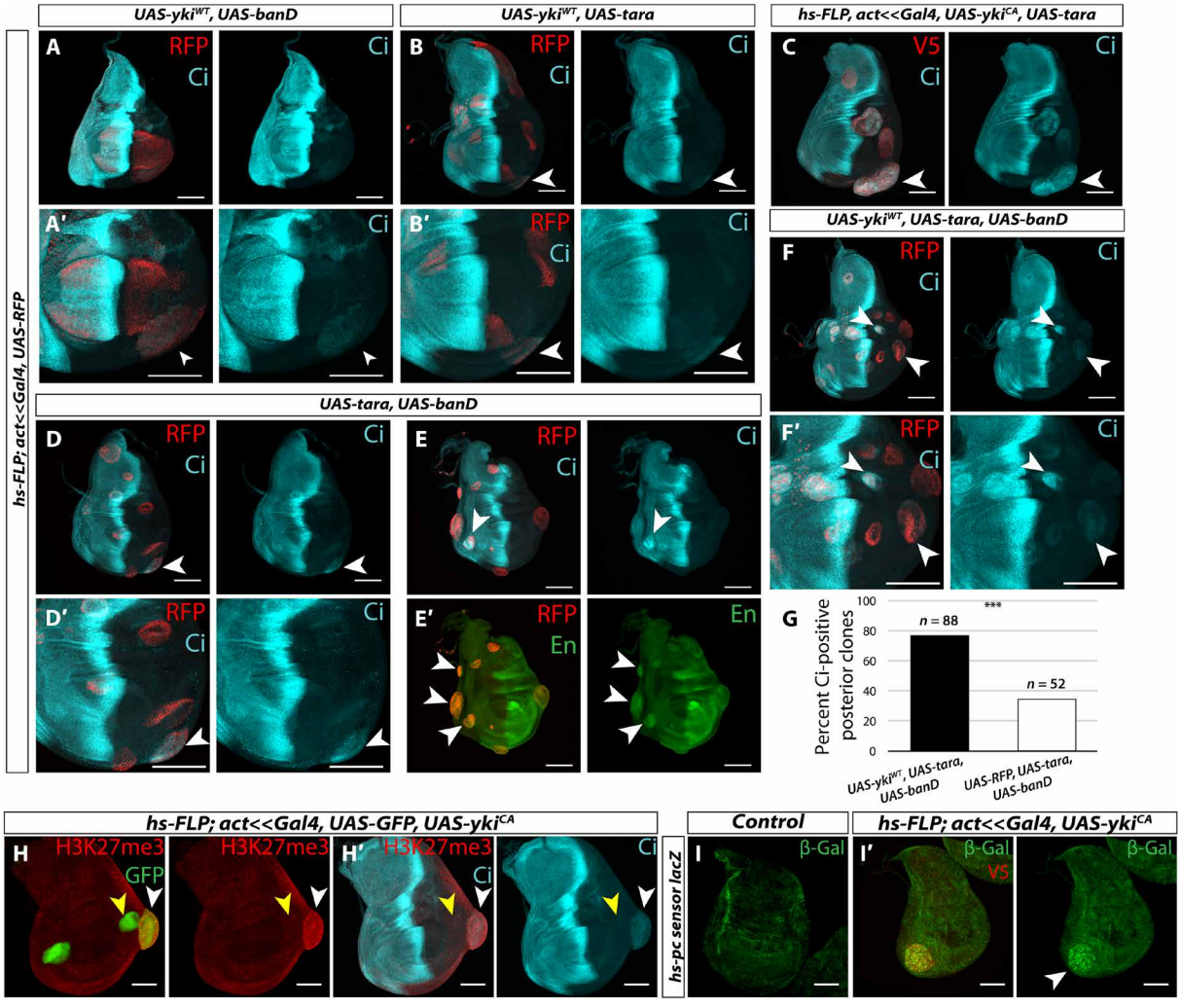

Fig. 3. *ban* and *tara* in combination induce ectopic patterning gene expression. (**A** and **B**) Hinge clones expressing either *banD* (A and A′) or tara (B and B′) together with yki^{WT} express Ci especially in the ventral hinge. (**C**) Overexpression of *tara* in yki^{CA} clones further increases Ci expression. (**D** and **E**) Combined expression of *ban* and *tara* causes some overgrowth and also Ci expression in posterior clones (D and D′) in increased Ci expression and ectopic En expression in anterior clones (E and E′). (**F** and **F′**) Clones expressing yki^{WT}, *ban*, and *tara* are more overgrown than yki^{WT} alone or with *ban* or *tara* individually and consistently express ectopic Ci in the posterior compartment. (**G**) A total of 77.3% of posterior clones expressing yki^{WT}, *tara*, and *ban* express ectopic Ci, while 34.6% of posterior clones expressing *RFP*, *tara*, and *ban* are Ci positive. (**H** and **H′**) yki^{CA} clones (GFP positive) show increased H3K27 trimethylation (H3K27me3; red) (H). This increase is only seen in clones in the hinge, where H3K27me3 is already higher than the rest of the disc (white arrowhead) and not in the pouch (yellow arrowhead). (H′) Increased H3K27me3 coincides with ectopic Ci expression. (**I** and **I′**) yki^{CA} clones show decreased Pc-mediated repression of a Polycomb-responsive element from the *bxd* locus linked to a *lacZ* reporter (green). Yki^{CA} was tagged with V5. Statistics: See Materials and Methods.

in other overgrown tissue, we stained discs with clones expressing either *RasV12* or *Myc* with antibodies that recognize Tara and H3K27me3. Neither *RasV12*- nor *Myc*-expressing clones showed changes in Tara or H3K27me3 relative to surrounding wild-type tissue (fig. S4, E and F), supporting the conclusion that these changes in chromatin regulation are specific to Yki^{CA} activation.

What are the consequences of creating yki^{CA} clones that have down-regulated *en* and express *ci* in the posterior compartment? The juxtaposition of cells that express *en* and those that do not normally occurs at the anteroposterior compartment boundary. *ci* is expressed in anterior cells but repressed by En in posterior cells, which instead secrete the short-range morphogen Hedgehog (Hh) (*40*). Activation of the Hh signaling pathway in cells anterior to the compartment boundary stabilizes the activator form of Ci and results in the transcription of multiple target genes including *patched* (*ptc*) and *dpp* (*41*, *42*). Dpp is a long-range morphogen that diffuses widely from its source and regulates tissue growth and gene expression in both compartments (*43*, *44*). We found that the presence of Ci-expressing yki^{CA} clones in the posterior compartment generates ectopic sites of Hh pathway signaling near the clone boundary, possibly due to increased levels of the full-length activator form of Ci. The Hh target genes *dpp* and *ptc* were both expressed in these clones (Fig. 4, A and B). Evidence of Dpp signaling, as assessed with the presence of the phosphorylated form of the signaling protein Mad (pMAD), was also observed (Fig. 4C). This is noteworthy given previous results showing that Mad and Yki cooperate to activate *ban* (*45*), which we demonstrated is necessary for ectopic Ci activation (Fig. 2, K to M and R). Thus, the clone boundary has indeed adopted anteroposterior

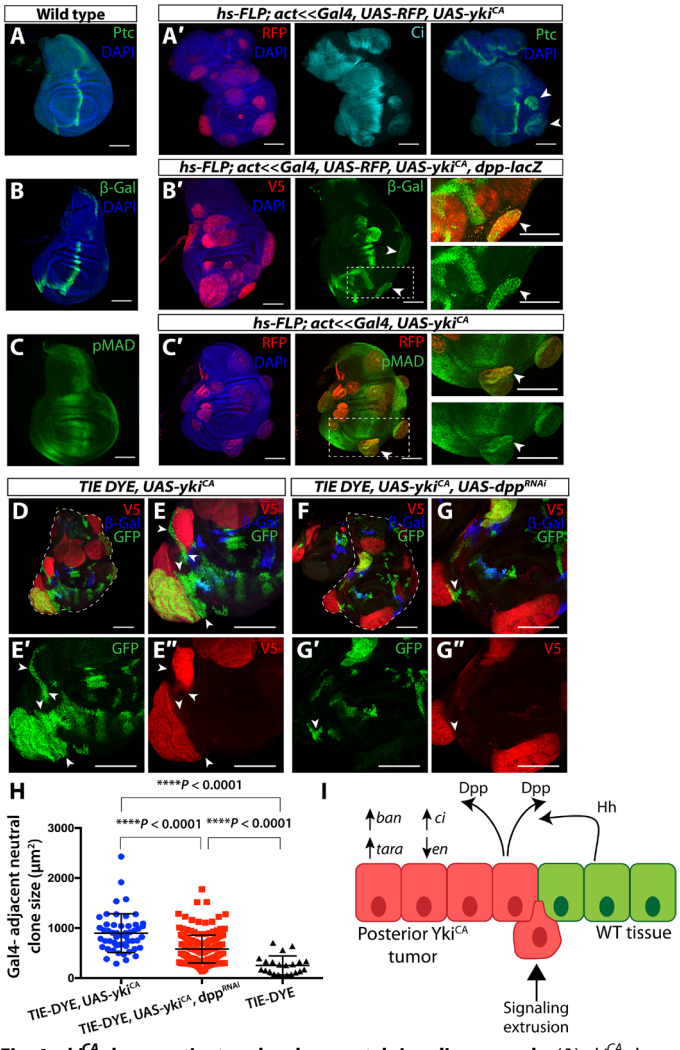

Fig. 4. *yki*^{CA} clones activate a developmental signaling cascade. (**A**) *yki*^{CA} clones that express Ci also express Ptc (**A′**) and *dpp-lacZ* (**B′**) at clone margin and have increased pMAD near clones (**C′**). Control discs without *yki*^{CA} clones are shown in (A) to (C). (**D** and **E**) *yki*^{CA} clones cause nonautonomous overgrowth in neighboring WT tissue. The TIE-DYE system has three independent FLP-out transgenes that express Gal4, GFP, and *lacZ*. Clones might express none of these or any combination of these depending on the number of FLP-out events in founder cells. Gal4-expressing clones express *UAS-yki*^{CA} and are visualized with anti-V5. Neutral GFP-expressing clones are shown in green, and lacZ-expressing clones are shown in blue. Arrowheads indicate two unusually large GFP-positive WT clones that are immediately adjacent to overgrown Yki^{CA}-expressing clones (red). (**F** and **G**) Knockdown of *dpp* in *yki*^{CA} clones. In these discs, neutral clones adjacent to *yki*^{CA} clones are not as overgrown (arrowheads). (**H**) Quantification of size of neutral clones directly adjacent to Gal4-expressing clones [expressing *UAS-yki*^{CA} (neutral clone, $n = 52$), *UAS-yki*^{CA} and *UAS-dpp*^{RNAi} (neutral clone, $n = 184$), or *UAS-RFP* (neutral clone, $n = 22$)]. (**I**) Model: Yki^{CA} causes changes in selector gene expression in the posterior compartment via up-regulation of *ban* and *tara*. As a result of heterotypic interactions at clone boundaries, ectopic organizing centers are created resulting in the production of morphogens (e.g., Dpp), as well as extrusion of *yki*^{CA} tissue. Statistics: See Materials and Methods.

compartment-boundary–like properties, at least with respect to Hh signaling. However, we did not see consistent evidence of clones establishing ectopic dorsoventral compartment boundaries. We did, however, observe some abnormalities in the pattern of dorsoventral gene expression (fig. S5, A to C). Some dorsal clones had reduced *apterous* expression (fig. S5C′, arrow), and some ventral clones expressed *cut* (fig. S5B′), which is normally expressed at the dorsoventral compartment boundary. However, in these ventral clones, *cut* was expressed throughout the clone and not at the boundary.

What are the consequences of activating Hh signaling in *yki*^{CA} clones? When we inactivated *smo* in *yki*^{CA} clones, we found no impairment in growth, nor did we find growth impairment when we reduced Ci itself in *yki*^{CA} clones (fig. S5, D to F and I). We also observed no significant difference in anterior versus posterior clone size for *yki*^{CA} clones, *smo*^{3}, *yki*^{CA} clones, or *yki*^{CA}, *ci*^{RNAi} clones (fig. S5, G, H, and J). Thus, their overgrowth is not dependent on Hh signaling. This is consistent with the obvious overgrowth observed in *yki*^{CA} clones far from the compartment boundary in the anterior compartment, which are also far from an Hh source. Since the clones were overgrown and in the process of extrusion, it was difficult to ascertain whether clones close to the compartment boundary had crossed it (fig. S5F). Clone overgrowth and changes in selector gene expression were also not dependent on c-Jun N-terminal kinase pathway activation, which has been previously linked to Hippo pathway signaling and thought to facilitate propagation of Yki activity to cells neighboring tumor cells (fig. S5, K to N) (*46*–*49*). To investigate potential nonautonomous effects of *yki*^{CA} clones, we used the TIE-DYE system (*50*), which has three independent FLP-out genes, two of which, when activated, express reporters driven by constitutive promoters (*ubi-GFP* and *act-lacZ*). The third is a FLP-out Gal4; these clones express *UAS-yki*^{CA}. While *yki*^{CA}-expressing clones are obviously overgrown, we also observed occasional large neutral clones that appeared to be composed of cells that were close to the perimeter of the *yki*^{CA}-expressing clones, including anterior clones that have elevated full-length Ci (Figs. 1C′ and 4, D and E). These clones were not as evident when a *UAS-dpp*^{RNAi} transgene was coexpressed with *yki*^{CA}. Neutral clones adjacent to *yki*^{CA}-expressing clones were significantly larger than those adjacent to *yki*^{CA}, *dpp*^{RNAi}–expressing clones (Fig. 4, F to H, and fig. S5O). This suggests that Dpp secreted by *yki*^{CA} clones may be able to promote the growth of adjacent cells, especially in lateral regions of the disc (Fig. 4I).

DISCUSSION

Human cancers are characterized by multiple genetic lesions, a subset of which are driver mutations that are thought to be responsible for their tumorous characteristics. It is estimated that most cancers have two to eight driver mutations (*5*). This makes it difficult to evaluate the contribution of each mutation to any particular characteristic of the tumor. We have taken advantage of the ability of single-gene manipulations to cause overgrowth in *Drosophila* imaginal discs to assess the ability of three different oncogenes to destabilize established patterns of selector gene expression and find that *yki*, the *Drosophila* ortholog of Yap and Taz, is especially potent in doing so. The patterns of expression of En, Ci, and Ubx are established relatively early in embryogenesis and maintained stably in imaginal discs during the larval stages of development. These patterns of expression can be disrupted in clones expressing an activated form of Yki. Expression of a wild-type form of Yki is capable of disrupting these expression patterns in combination with other genetic manipulations such as overexpression of *ban* or *tara*. This latter scenario is more likely to apply to human cancers; increased Yap or Taz activity has been described in multiple human cancers (*51*), which often also have other genetic lesions.

Our studies show that *sd*, *ban*, and *tara* make important contributions to the pathway by which Yki^{CA} destabilizes gene expression; reducing the expression of any of these in clones expressing Yki^{CA} greatly reduces ectopic Ci expression, and increasing expression of both genes can cause ectopic Ci expression. It is likely that other mechanisms function in parallel to destabilize selector gene expression since combined overexpression of *ban* and *tara* increased ectopic Ci expression but did not reduce En expression.

We also demonstrate that changing selector gene expression within an overgrowing clone can create interactions at the clone margin that are reminiscent of compartment boundaries and result in the production of morphogens. A recent study showed that forced expression of En in *lgl* clones can elicit similar phenomena in anterior clones (*52*). In addition, yki^{CA} clones are often extruded, consistent with previous observations that heterotypic interactions caused by overexpressing patterning genes also promotes extrusion (*14*–*16*). Previous work found that *ci* RNA levels were increased in *wts* mutant tissue (*25*), yet we did not see ectopic Ci protein expression in *wts* mutant clones or wild-type Yki-overexpressing clones. Our work shows therefore that sustained expression of very high Yki levels is necessary to destabilize expression of selector genes. However, even under these conditions, the effect on ectopic Ci expression is Sd dependent. Moreover, we have shown that even wild-type Yki can, in combination with increased expression of *ban* or *tara*, induce ectopic Ci expression. While these changes in gene expression are most obvious with above-physiological levels of Yki, they nevertheless reflect a previously unknown ability of this pathway to alter patterning gene expression and furthermore to change the growth characteristics of neighboring wild-type cells. Differences in selector gene expression between human cancers or precancerous lesions and their wild-type neighbors have received relatively little attention, and our results call attention to tumor margins as sites where heterotypic interactions could create signaling centers that affect the behavior of tumor cells.

MATERIALS AND METHODS

Experimental design

We set out to characterize the ectopic expression of selector genes seen in some overgrown tissues and to investigate the role of this ectopic gene expression in the biology of overgrowth. To generate overgrown tissue, we used a system with heat shock–induced FLPase and actin-driven FLP-out Gal4 with $UAS\text{-}yki^{S168A}$. This system generated random overgrown clones throughout the larva, with clone frequency controlled by length of heat shock. All components of this system were contained within one stable stock that could be crossed to other stocks to test the role of candidate genes and use lacZ reporters.

Drosophila stocks

Stocks used in this study include the following: *hsFLP; act<stop<Gal4, UAS-yki*^{S168A}.v5, *hsFLP;act<stop<Gal4, UAS-RFP*^{NLS}, *hsFLP, UAS-GFP*^{NLS}; *tub-Gal80, FRT40A (MARCM FRT 40A), ubi>RFP, FRT40A, banΔ1, banGFP, en-Gal4, dpp-lacZ, UAS-RFP, AP-1-RFP* (*53*), and TIE-DYE (*50*). Stocks were obtained from the Bloomington Drosophila Stock Center (BDSC): *UAS-yki*^{S168A}*.v5* (#28818), *UAS-yki.v5* (#28819), *UAS-yki::GFP* (#28815), wts^{X1} (#44251), smo^{3} (#3277), *UAS-ci*^{RNAi} (#64928), *tara1-lacZ* (#6403), *UAS-tara*^{RNAi} (#31634), *nub-Gal4* (#42699), *30A-Gal4* (#37534), *UAS-dMyc* (#9674), *UAS-rasv12* (#4847), and *UAS-jnk*^{DN} (#9311). *Ci-lacZ* was a gift from D. Kalderon (Columbia University, USA). *UAS-bantam*^{sponge} and *UAS-bantam.D* were gifts from S. Cohen (University of Copenhagen, Denmark). hs-Pc-sensor was a gift from V. Pirrotta (Rutgers University, USA). *UAS-myc::tara* was a gift from R. Smith-Bolton [University of Illinois, Urbana-Champaign, USA (originally from M. Cleary, University of California, Merced, USA)]. *MARCM FRT19A* and sd^{47M}, *FRT19A* were gifts from D. Pan.

Temperature shift and clone induction experiments

Experiments using heat shock–controlled FLPase and *act<<Gal4* were maintained at 25°C, heat shocked for 7 min at 37°C at 72 hours after egg lay (hAEL) ± 12 hours, and then dissected and analyzed at 144 hAEL ± 12 hours. TIE-DYE experiments were conducted under the same conditions. Because ascertaining clone boundaries in this system can be challenging, we attempted to score only clones where boundaries were reasonably clear. hsFLP-induced mosaic analysis with a repressible cell marker (MARCM) experiments were conducted under the same conditions but with 10- to 15-min heat shocks (except for MARCM 19A experiments in Fig. 2, which were heat shocked for 1 hour). Discs in fig. S5D were dissected at 120 hAEL because of the lack of developmental delay in these larvae, while larvae expressing yki^{CA} are delayed by approximately 1 day and thus were dissected at 144 hAEL. Crosses using *nub-Gal4*, *30A-Gal4*, and *en-Gal4* were incubated at 25°C, and larvae were dissected at wandering third instar (approximately 120 to 144 hAEL).

Immunohistochemistry

Imaginal discs were dissected and fixed in 4% paraformaldehyde for 20 min, washed and permeabilized in phosphate-buffered saline with 0.1% Triton X-100, and blocked in 10% normal goat serum. Primary antibodies used were α-Ci [1:25; Developmental Studies Hybridoma Bank (DSHB)], α-Ubx (1:10; DSHB), α-En (1:25; DSHB), α-β-galactosidase (1:500; Promega), α-V5 (1:500; Sigma-Aldrich), α-Wg (1:100; DSHB), α-Cut (1:100), α-Ptc (1:50; DSHB), α-pMAD (1:500; Abcam), α-Smo (1:10; DSHB), α-MMP1 (1:100; a combination of 14A3D2, 3A6B4, and 5H7B11; DSHB), α-Tara (1:700; K. Koh), α-H3K27me3 (1:500; Active Motif), α-H3K9me3 (1:500; Active Motif), α-H3K4me1 (1:500; Active Motif), α-H3K4me3 (1:500; Active Motif), α-H4ac (1:500; Active Motif), and α-Sd (1:500; K. Guss). Secondary antibodies were from Cell Signaling Technology and used at 1:400. Nuclei were stained with 4′,6-diamidino-2-phenylindole (1:1000; Cell Signaling Technology). Samples were imaged on a Zeiss LSM 700 confocal microscope.

Statistical analysis

Images were processed using Fiji (*54*), and statistical analysis was completed with GraphPad Prism and VassarStats 2x2 Contingency Table. All scale bars are 100 μm unless otherwise noted. For clone size comparisons in Figs. 2K and 4H, *P* values were generated through a one-way analysis of variance (ANOVA) with Tukey's multiple comparison test for wild-type clones, yki^{CA} clones in a wild-type background, yki^{CA} clones in a $ban^{\Delta 1}$/+ background, and yki^{CA} clones with $tara^{RNAi}$ (2K) or TIE-DYE yki^{CA} clones, TIE-DYE yki^{CA}, dpp^{RNAi} clones, or TIE-DYE wild-type clones (4H). Error bars are SDs. All comparisons between wild-type clones and other conditions had a *P* value of <0.0001. For comparisons of the rate of Ci-positive posterior clones in Figs. 2L and 3D, Yates *P* values were calculated with a χ^2 test. All are <0.0001 except yki^{CA} compared to yki^{CA}, $ban^{\Delta 1}$/+ total clones, which is 0.0009. ***$P < 0.001$, very significant; **$P = 0.001$

to 0.01, very significant; *P = 0.01 to 0.05, significant; $P > 0.05$, not significant. Anterior versus posterior clone size comparisons in fig. S5 (G, H, and J) P values were calculated with an unpaired Student's t test in GraphPad.

SUPPLEMENTARY MATERIALS

Supplementary material for this article is available at http://advances.sciencemag.org/cgi/content/full/6/50/eabe8159/DC1

View/request a protocol for this paper from *Bio-protocol*.

REFERENCES AND NOTES

1. R. J. Britten, E. H. Davidson, Gene regulation for higher cells: A theory. *Science* **165**, 349–357 (1969).
2. C. D. Allis, T. Jenuwein, The molecular hallmarks of epigenetic control. *Nat. Rev. Genet.* **17**, 487–500 (2016).
3. J. B. Axelsen, J. Lotem, L. Sachs, E. Domany, Genes overexpressed in different human solid cancers exhibit different tissue-specific expression profiles. *Proc. Natl. Acad. Sci. U.S.A.* **104**, 13122–13127 (2007).
4. W. A. Flavahan, E. Gaskell, B. E. Bernstein, Epigenetic plasticity and the hallmarks of cancer. *Science* **357**, eaal2380 (2017).
5. B. Vogelstein, N. Papadopoulos, V. E. Velculescu, S. Zhou, L. A. Diaz Jr., K. W. Kinzler, Cancer genome landscapes. *Science* **339**, 1546–1558 (2013).
6. J. A. Kassis, J. A. Kennison, J. W. Tamkun, Polycomb and Trithorax group genes in *Drosophila*. *Genetics* **206**, 1699–1725 (2017).
7. L. A. Johnston, D. A. Prober, B. A. Edgar, R. N. Eisenman, P. Gallant, *Drosophila* myc regulates cellular growth during development. *Cell* **98**, 779–790 (1999).
8. D. A. Prober, B. A. Edgar, Ras1 promotes cellular growth in the *Drosophila* wing. *Cell* **100**, 435–446 (2000).
9. F. D. Karim, G. M. Rubin, Ectopic expression of activated Ras1 induces hyperplastic growth and increased cell death in Drosophila imaginal tissues. *Development* **125**, 1–9 (1998).
10. J. Huang, S. Wu, J. Barrera, K. Matthews, D. Pan, The Hippo signaling pathway coordinately regulates cell proliferation and apoptosis by inactivating Yorkie, the *Drosophila* homolog of YAP. *Cell* **122**, 421–434 (2005).
11. C. M. Pfleger, The Hippo pathway: A master regulatory network important in development and dysregulated in disease. *Curr. Top. Dev. Biol.* **123**, 181–228 (2017).
12. J. Dong, G. Feldmann, J. Huang, S. Wu, N. Zhang, S. A. Comerford, M. F. Gayyed, R. A. Anders, A. Maitra, D. Pan, Elucidation of a universal size-control mechanism in *Drosophila* and mammals. *Cell* **130**, 1120–1133 (2007).
13. H. Oh, K. D. Irvine, In vivo regulation of Yorkie phosphorylation and localization. *Development* **135**, 1081–1088 (2008).
14. M. C. Gibson, N. Perrimon, Extrusion and death of DPP/BMP-compromised epithelial cells in the developing *Drosophila* wing. *Science* **307**, 1785–1789 (2005).
15. J. Shen, C. Dahmann, Extrusion of cells with inappropriate Dpp signaling from *Drosophila* wing disc epithelia. *Science* **307**, 1789–1790 (2005).
16. C. Bielmeier, S. Alt, V. Weichselberger, M. La Fortezza, H. Harz, F. Jülicher, G. Salbreux, A.-K. Classen, Interface contractility between differently fated cells drives cell elimination and cyst formation. *Curr. Biol.* **26**, 563–574 (2016).
17. Y. Tamori, E. Suzuki, W.-M. Deng, Epithelial tumors originate in tumor hotspots, a tissue-intrinsic microenvironment. *PLOS Biol.* **14**, e1002537 (2016).
18. S. Verghese, T. T. Su, Drosophila Wnt and STAT define apoptosis-resistant epithelial cells for tissue regeneration after irradiation. *PLOS Biol.* **14**, e1002536 (2016).
19. S. Eaton, T. B. Kornberg, Repression of ci-D in posterior compartments of Drosophila by engrailed. *Genes Dev.* **4**, 1068–1077 (1990).
20. C. Schwartz, J. Locke, C. Nishida, T. B. Kornberg, Analysis of cubitus interruptus regulation in Drosophila embryos and imaginal disks. *Development* **121**, 1625–1635 (1995).
21. G. Chanas, S. Lavrov, F. Iral, G. Cavalli, F. Maschat, Engrailed and *polyhomeotic* maintain posterior cell identity through *cubitus-interruptus* regulation. *Dev. Biol.* **272**, 522–535 (2004).
22. N. H. Patel, E. Martin-Blanco, K. G. Coleman, S. J. Poole, M. C. Ellis, T. B. Kornberg, C. S. Goodman, Expression of *engrailed* proteins in arthropods, annelids, and chordates. *Cell* **58**, 955–968 (1989).
23. R. S. Mann, Engrailed-mediated repression of Ultrabithorax is necessary for the parasegment 6 identity in Drosophila. *Development* **120**, 3205–3212 (1994).
24. B. S. Emerald, L. S. Shashidhara, Negative regulation of *Ultrabithorax* expression by *engrailed* is required for proper specification of wing development in *Drosophila melanogaster*. *J. Genet.* **79**, 61–70 (2000).
25. H. Oh, M. Slattery, L. Ma, A. Crofts, K. P. White, R. S. Mann, K. D. Irvine, Genome-wide association of Yorkie with chromatin and chromatin-remodeling complexes. *Cell Rep.* **3**, 309–318 (2013).
26. Y. Goulev, J. D. Fauny, B. Gonzalez-Marti, D. Flagiello, J. Silber, A. Zider, SCALLOPED interacts with YORKIE, the nuclear effector of the hippo tumor-suppressor pathway in *Drosophila*. *Curr. Biol.* **18**, 435–441 (2008).
27. J. Yu, D. Pan, Validating upstream regulators of Yorkie activity in Hippo signaling through *scalloped*-based genetic epistasis. *Development* **145**, dev157545 (2018).
28. J. Brennecke, D. R. Hipfner, A. Stark, R. B. Russell, S. M. Cohen, bantam encodes a developmentally regulated microRNA that controls cell proliferation and regulates the proapoptotic gene *hid* in *Drosophila*. *Cell* **113**, 25–36 (2003).
29. B. J. Thompson, S. M. Cohen, The Hippo pathway regulates the bantam microRNA to control cell proliferation and apoptosis in *Drosophila*. *Cell* **126**, 767–774 (2006).
30. R. Nolo, C. M. Morrison, C. Tao, X. Zhang, G. Halder, The *bantam* MicroRNA is a target of the hippo tumor-suppressor pathway. *Curr. Biol.* **16**, 1895–1904 (2006).
31. D. R. Hipfner, K. Weigmann, S. M. Cohen, The bantam gene regulates Drosophila growth. *Genetics* **161**, 1527–1537 (2002).
32. H. Herranz, X. Hong, S. M. Cohen, Mutual repression by bantam miRNA and capicua links the EGFR/MAPK and Hippo pathways in growth control. *Curr. Biol.* **22**, 651–657 (2012).
33. S. Calgaro, M. Boube, D. L. Cribbs, H.-M. Bourbon, The Drosophila gene taranis encodes a novel trithorax group member potentially linked to the cell cycle regulatory apparatus. *Genetics* **160**, 547–560 (2002).
34. K. J. Schuster, R. K. Smith-Bolton, Taranis protects regenerating tissue from fate changes induced by the wound response in *Drosophila*. *Dev. Cell* **34**, 119–128 (2015).
35. P. Dutta, W. X. Li, The SERTAD protein Taranis plays a role in Polycomb-mediated gene repression. *PLOS ONE* **12**, e0180026 (2017).
36. J. Müller, C. M. Hart, N. J. Francis, M. L. Vargas, A. Sengupta, B. Wild, E. L. Miller, M. B. O'Connor, R. E. Kingston, J. A. Simon, Histone methyltransferase activity of a *Drosophila* Polycomb group repressor complex. *Cell* **111**, 197–208 (2002).
37. E. Viré, C. Brenner, R. Deplus, L. Blanchon, M. Fraga, C. Didelot, L. Morey, A. Van Eynde, D. Bernard, J.-M. Vanderwinden, M. Bollen, M. Esteller, L. D. Croce, Y. de Launoit, F. Fuks, The Polycomb group protein EZH2 directly controls DNA methylation. *Nature* **439**, 871–874 (2005).
38. Y. Cheng, A. L. Brunner, S. Kremer, S. K. DeVido, C. M. Stefaniuk, J. A. Kassis, Co-regulation of *invected* and *engrailed* by a complex array of regulatory sequences in Drosophila. *Dev. Biol.* **395**, 131–143 (2014).
39. G. I. Dellino, Y. B. Schwartz, G. Farkas, D. McCabe, S. C. R. Elgin, V. Pirrotta, Polycomb silencing blocks transcription initiation. *Mol. Cell* **13**, 887–893 (2004).
40. T. Tabata, S. Eaton, T. B. Kornberg, The Drosophila hedgehog gene is expressed specifically in posterior compartment cells and is a target of engrailed regulation. *Genes Dev.* **6**, 2635–2645 (1992).
41. T. Von Ohlen, D. Lessing, R. Nusse, J. E. Hooper, Hedgehog signaling regulates transcription through cubitus interruptus, a sequence-specific DNA binding protein. *Proc. Natl. Acad. Sci. U.S.A.* **94**, 2404–2409 (1997).
42. P. Aza-Blanc, F.-A. Ramírez-Weber, M.-P. Laget, C. Schwartz, T. B. Kornberg, Proteolysis that is inhibited by hedgehog targets Cubitus interruptus protein to the nucleus and converts it to a repressor. *Cell* **89**, 1043–1053 (1997).
43. D. Nellen, R. Burke, G. Struhl, K. Basler, Direct and long-range action of a Dpp morphogen gradient. *Cell* **85**, 357–368 (1996).
44. T. Lecuit, W. J. Brook, M. Ng, M. Calleja, H. Sun, S. M. Cohen, Two distinct mechanisms for long-range patterning by Decapentaplegic in the *Drosophila* wing. *Nature* **381**, 387–393 (1996).
45. H. Oh, K. D. Irvine, Cooperative regulation of growth by Yorkie and mad through *bantam*. *Dev. Cell* **20**, 109–122 (2011).
46. X. Ma, H. Wang, J. Ji, W. Xu, Y. Sun, W. Li, X. Zhang, J. Chen, L. Xue, Hippo signaling promotes JNK-dependent cell migration. *Proc. Natl. Acad. Sci. U.S.A.* **114**, 1934–1939 (2017).
47. V. A. Codelia, G. Sun, K. D. Irvine, Regulation of YAP by mechanical strain through Jnk and Hippo signaling. *Curr. Biol.* **24**, 2012–2017 (2014).
48. M. Enomoto, T. Igaki, Src controls tumorigenesis via JNK-dependent regulation of the Hippo pathway in *Drosophila*. *EMBO Rep.* **14**, 65–72 (2013).
49. M. Enomoto, D. Kizawa, S. Ohsawa, T. Igaki, JNK signaling is converted from anti- to pro-tumor pathway by Ras-mediated switch of Warts activity. *Dev. Biol.* **403**, 162–171 (2015).
50. M. I. Worley, L. Setiawan, I. K. Hariharan, TIE-DYE: A combinatorial marking system to visualize and genetically manipulate clones during development in *Drosophila melanogaster*. *Development* **140**, 3275–3284 (2013).
51. F. Zanconato, M. Cordenonsi, S. Piccolo, YAP/TAZ at the roots of cancer. *Cancer Cell* **29**, 783–803 (2016).
52. A. Bajpai, P. Sinha, Hh signaling from *de novo* organizers drive *lgl* neoplasia in *Drosophila* epithelium. *Dev. Biol.* **457**, 1–8 (2020).
53. N. Chatterjee, D. Bohmann, A versatile φC31 based reporter system for measuring AP-1 and NRF2 signaling in *Drosophila* and in tissue culture. *PLOS ONE* **7**, e34063 (2012).

54. J. Schindelin, I. Arganda-Carreras, E. Frise, V. Kaynig, M. Longair, T. Pietzsch, S. Preibisch, C. Rueden, S. Saalfeld, B. Schmid, J.-Y. Tinevez, D. J. White, V. Hartenstein, K. Eliceiri, P. Tomancak, A. Cardona, Fiji: An open-source platform for biological-image analysis. *Nat. Methods* **9**, 676–682 (2012).

Acknowledgments: We thank members of the Hariharan Lab for helpful discussion and suggestions; L. Setiawan and M. Worley for feedback on the manuscript; H. Mazdeyasna for experimental assistance; D. Kalderon, S. Cohen, V. Pirrotta, R. Smith-Bolton, D. Pan, and the BDSC for fly stocks; K. Koh for the anti-Taranis antibody; and K. Guss for the anti-Sd antibody. **Funding:** This work was funded by a grant to I.K.H. from the NIH (R35 GM122490) and a Research Professor Award from the American Cancer Society (RP-16-238-06-COUN). **Author contributions:** J.C.D.B., M.E.-B., and I.K.H. designed and interpreted experiments. J.C.D.B. and M.E.-B. conducted experiments. J.C.D.B. and M.E.-B. prepared the figures. J.C.D.B. and I.K.H. wrote the paper.

Competing interests: The authors declare that they have no competing interests. **Data and materials availability:** All data needed to evaluate the conclusions in the paper are present in the paper and/or the Supplementary Materials. Fly stocks generated for this paper may be obtained upon request. Additional data related to this paper may be requested from the authors.

Submitted 16 September 2020
Accepted 22 October 2020
Published 9 December 2020
10.1126/sciadv.abe8159

Citation: J. C. D. Bairzin, M. Emmons-Bell, I. K. Hariharan, The Hippo pathway coactivator Yorkie can reprogram cell fates and create compartment-boundary–like interactions at clone margins. *Sci. Adv.* **6**, eabe8159 (2020).